Hospital and urban wastewaters shape the structure and active resistome of environmental biofilms

Elena Buelow[1,2], Catherine Dauga[3,4*], Claire Carrion[5], Hugo Mathé-Hubert[1], Sophia Achaibou [4], Margaux Gaschet[2], Thomas Jové[2], Olivier Chesneau[6], Sean P. Kennedy[3], Marie-Cecile Ploy[2], Sandra Da Re[2], Christophe Dagot[2]

1 Univ. Grenoble Alpes, CNRS, UMR 5525, VetAgro Sup, Grenoble INP, TIMC, 38000 Grenoble, France

2 INSERM, CHU Limoges, RESINFIT, UMR1092, University of Limoges, Limoges, France

3 Institut Pasteur, Université Paris Cité, Département Biologie Computationnelle, F-75015 Paris, France

4 Biomics Pole, CITECH, Institut Pasteur, F-75015 Paris, France

5 University of Limoges, INSERM; CHU Limoges, UMR CNRS 7276, F-87000 Limoges, France

6 Collection de l'Institut Pasteur (CIP), Microbiology Department, Institut Pasteur, Paris 75015, France

* present address: Institut Pasteur, University Paris Cité, Department of Virology, Arboviruses and Insect Vectors, F-75015 Paris, France

Abstract

We studied hospital and urban wastewater (WW) biofilms *in situ* and in an *in vitro* laboratory model to assess and compare their potential to actively disseminate and express antibiotic resistance genes (ARGs). Biofilms were subjected to confocal microscopy to qualify and quantify their extracellular polymeric substances (EPSs), including polysaccharides, external DNA (eDNA), and lipids. We observed that antibiotic challenge had a differential impact on the EPS and the live-dead ratios of *in vitro* hospital and urban WW biofilms. Differential expression of a range of ARGs and mobile genetic elements (MGEs), including those on plasmids, was assessed using a meta-transcriptomic approach. Expression of ARGs as well as MGEs, *in situ,* was 10-fold higher in hospital WW biofilms compared with urban, suggesting a higher frequency of ARG transfer might occur in hospital WW. *In vitro* data confirmed that the addition of ciprofloxacin significantly increased ARG and MGE expression in hospital but not in urban WW biofilms suggesting that the regulation of ARG and MGE expression is likely dependent on the structure and composition of the biofilm. The different responses to antibiotic pressure in hospital *vs* urban biofilms, coupled with differences in biofilm structure helps delineate distinct characteristics of hospital and urban WW biofilms.

Introduction

Biofilms are the preferred lifestyle of bacteria in the natural environment. They present structures that support high densities of bacteria, exhibit high tolerance to antimicrobials, and facilitate gene transfer [1–3]. In aquatic environments, biofilms are suggested to serve as hot spots for the accumulation and dissemination of antimicrobial resistance genes (ARG) [1,4]. Chemical pollutants spread by urban, industrial, and agricultural waste exert a continuous selective pressure on the diverse antibiotic resistance gene (ARG) pool present in the natural environment and its microbial communities [5–7]. For example, ciprofloxacin is a very stable molecule often found in anthropogenically polluted environments and enriched in wastewater (WW), particularly hospital WW [7–10]. Ciprofloxacin is not efficiently removed by WW treatment through activated sludge [11]; it can be detected in WW and downstream aquatic environments and was identified to pose a significant risk for selection of antimicrobial resistance (AMR) in these environments [9,10,12]. Furthermore, ciprofloxacin is known to induce the SOS-response in Gram-negative bacteria. This induction of the SOS response can lead to the expression of antibiotic resistance genes as the quinolone resistance-encoding *qnrB* gene, or the expression of genetic elements as the class 1 integron integrase gene, leading to ARG cassette rearrangements [13,14]. In addition, bacteria that are present in the human gut carry a wide variety of ARGs that can be spread into the environment by human feces through WW [15–18]. To limit the dissemination of chemical pollutants, pathogens and ARGs into the environment, the implementation of WW treatment systems worldwide plays a key role [6,19–21]. However, WW treatment plants are also regarded as selection and dissemination hot spots due to the high density of human gut, environmental bacteria, and chemical pollutants [22–24]. Biofilms in WW systems represent an important source of ARGs and bacteria that may end up circulating in the environment and hence present an important model to study the dissemination of resistance in the context of discharged effluents [4,25,26]. Biofilms dominate most habitats on earth, accounting for ~ 80% of all bacterial and archaeal cells [27]. Biofilm communities are typified by high densities of bacteria embedded in a self-produced protective matrix, which contributes to high antibiotic tolerance, and facilitates gene transfer [4,28]. Extracellular polymeric substances (EPS), such as external DNA (eDNA), proteins, lipids, and polysaccharides, are essential structural components of the biofilm matrix that are involved in resilience to antibiotics and exogenous stress, but also in horizontal gene transfer (HGT) [29–31]. Previous studies have shown that hospital WW contain significantly higher amounts of resistant bacteria, ARGs and mobile genetic elements (MGEs), as well as chemical and pharmaceutical pollutants compared to urban WW. However, these quantities are generally diluted when hospital WW is mixed with urban WW in community sewer systems [7,32,33].

61 Demonstration of the transfer, dynamics, and regulation of ARGs and MGEs in a complex environmental
62 matrix is yet experimentally challenging, with many essential open questions such as how and when
63 transfer and dissemination of ARGs occur in nature. The extent and conditions of MGE transfer that carry
64 ARGs is still largely unexplored in natural environments and microbial communities. In this study we
65 implemented a sampling and analysis approach that allows phenotypic and genomic analyses of *in situ*
66 and reconstituted *in vitro* hospital and urban wastewater (WW) biofilms. To better understand the role of
67 hospital and urban WW biofilms in effectively disseminating antimicrobial resistance in the WW system,
68 we explored the extracellular polymeric substances (EPS) within the biofilm matrix, the composition of
69 the biofilm community (microbiota), the resistome (antibiotic, biocide, and heavy metal resistance genes)
70 and mobilome (mobile genetic elements), with focus on expressed genes (metatranscriptome).

71 **Materials and Methods**

72 **Sample collection and biofilm production *in situ* and *in vitro*:**

73 Wastewater (WW) biofilm production campaigns (*in vitro* and *in situ*) were conducted in January 2017.
74 For *in vitro* biofilms, 20L of untreated urban (up flow of the WWTP Limoges city), and hospital (900-bed,
75 Limoges teaching hospital France) WW were collected on the same day and transported (at 4°C) to the
76 laboratory for immediate use in continuous biofilm reactors. The remaining WW was stored at 4°C to
77 replace evaporated volume every two days. For each WW type, two reactors containing 3L of WW were
78 fed at a continuous rate, from an external container containing the same WW (5L in total), ensuring
79 circulation and a stable level in the biofilm reactors (closed continuous system) (Supplementary Figure 1).
80 Rooms were kept darkened, and the temperature was maintained at 17°C. Sixteen polystyrene slides
81 suitable for confocal laser scanning microscopy (CLSM) (Agar Scientific LTD, UK) were attached to a rotator
82 that was constantly turning, producing 16 biological replicate biofilms per reactor. After 3 days of initial
83 biofilm formation, 1µg/L of ciprofloxacin (considered as the minimum selective concentration (MSC) of
84 ciprofloxacin for most environmental bacteria [34] was added to one reactor for each biofilm type (urban,
85 hospital, lab duplicate). On day 7, the urban and hospital biofilms grown in the reactors containing
86 ciprofloxacin were challenged with a fresh dose of ciprofloxacin (1 µg/L) and harvested the same day (D7)
87 4 hours after ciprofloxacin challenge. Samples were processed within 30 minutes after harvesting. For
88 metagenomics analysis, 8 biological replica biofilms were scraped with tissue cell scrapers (Biologix®) from
89 the slides and washed/suspended in 1X phosphate buffered saline solution (PBS), transferred in 2ml
90 Eppendorf tubes, and immediately shock frozen in liquid nitrogen. Samples were stored at -80°C until
91 RNA/DNA extraction. For CLSM analysis, the remaining 8 slides were washed gently once with 1x PBS and

92 either directly stained (for life/dead staining) or fixed in 3.7% formaldehyde solution for 1 hour and
93 preserved for subsequent EPS staining.

94 For *in situ* biofilms, holes were drilled into polystyrene slides ends and attached with fishing line (16 slides
95 in total, Supplementary Figure 1). The string of polystyrene slides was immersed into the hospital WW
96 pipe and attached at the access point. Slides were recovered after 7 days. Slides were separated and
97 carefully collected in a slide box containing cooled 1xPBS solution and transported to the laboratory
98 immediately for processing. Slides that showed sufficient biofilm formation (by eye) and were least
99 polluted with residues of tissue and other large waste debris, were immediately scraped from the slides
100 and shock frozen in liquid nitrogen as described above. Remaining slides were washed gently in 1xPBS and
101 fixed in 3.7% formaldehyde solution for 1 hour for subsequent EPS staining and CLSM analysis. The same
102 procedure was applied for the *in situ* biofilm production in the untreated urban WW directly at the WWTP
103 (slides were attached and emerged in the large WW receiving pipe/body after primary water filtration
104 step (removal of large debris)). Slides were recovered as described above and stored in a slide box
105 containing cooled 1xPBS. At least four suitable biofilm slides/replicates were directly processed on site by
106 scraping them from the slides and shock freezing them in a portable liquid nitrogen tank. The remaining
107 slides were transported at 4°C to the laboratory and fixed in 3.7% formaldehyde solution for subsequent
108 EPS staining and CLSM analysis as described below.

109 **Sample processing:**

110 DNA extraction was performed with the DNA/RNA dual extraction kit (Qiagen) according to the
111 manufacturer's instructions and stored at -20°C. RNA quality, as measured by RNA integrity number (RIN)
112 was insufficient for RNA sequencing. Therefore, RNA was extracted from remaining biological replicates
113 and samples using the ZymoBIOMICS DNA/RNA Miniprep Kit. DNA concentration was determined by
114 Qubit Fluorometric Quantitation (Thermo fisher scientific, Waltham, MA USA) assays according to the
115 manufacturer's instructions. All DNA samples were diluted or concentrated to a final concentration of 10
116 ng/µl for downstream qPCR and 16S rRNA analysis. RNA concentration and integrity were analyzed by the
117 Agilent 2100 Bioanalyzer system.

118 **16S rRNA gene sequencing and sequence data pre-processing**

119 Extracted DNA samples for 16S rRNA sequencing were prepared following a dual barcoded two-step PCR
120 procedure for amplicon sequencing for Illumina. The V4 region was sequenced by generating 2 x 300 bp

121 on an Illumina MiSeq. Data was demultiplexed and filtered for quality and remaining primers according to
122 recommended practices as described previously [7].

123 **16S rRNA data analysis**

124 Illumina MiSeq forward and reverse reads were processed using the MASQUE pipeline
125 (https://github.com/aghozlane/masque). Briefly, raw reads are filtered and combined followed by
126 dereplication (dereplication is the identification of unique sequences so that only one copy of each
127 sequence is reported) Chimera removal and clustering are followed by taxonomic annotation of the
128 resulting OTUs by comparison to the SILVA database. A BIOM file is generated that combines both OTU
129 taxonomic assignment and the number of matching reads for each sample. Relative abundance levels for
130 bacterial taxa (family/genus level) were obtained and analyzed [7].

131 **High-throughput qPCR for the characterization of the resistome composition and normalized**
132 **abundance:**

133 Nanolitre-scale quantitative PCRs to quantify genes that confer resistance to antimicrobials were
134 performed as described previously [7,32,35]. We targeted 76 genes, grouped into 16 resistance gene
135 classes; targeted genes include ARGs that are prevalent in the gut microbiota of healthy individuals [15],
136 clinically relevant ARGs (extended-spectrum β-lactamases (ESBLs), carbapenemases, and vancomycin
137 resistance), and heavy metals and quaternary ammonium compounds resistance genes suggested to favor
138 cross and co–selection for ARGs in the environment [36,37]. We also targeted 11 other targets, including
139 common transposase gene families and class 1, 2 and 3 integron integrase genes, that are important
140 vectors for ARGs in the clinics and often used as proxy for anthropogenic pollution [38]. This set of 87
141 genes constituted what we named the targeted resistome (Supplementary Table 1). We also included
142 primers targeting 16S rDNA. Primer design and validation prior to and after Biomark analysis has been
143 done as described earlier [7,35]. Real-Time PCR analysis was performed using the 96.96 BioMark™
144 Dynamic Array for Real-Time PCR (Fluidigm Corporation, San Francisco, CA, U.S.A) as described previously
145 (7). Thermal cycling and real-time imaging were performed at the Plateforme Génomique GeT – INRA
146 Transfert (https://get.genotoul.fr/en/), and Ct values were calculated using the BioMark Real-Time PCR
147 analysis software. Calculations for normalized and cumulative abundance of individual genes and
148 allocated gene classes were performed as previously described [7,32,35]. The resistome data displayed
149 here and used for statistical analysis is based on resistome data that was obtained for two biological
150 replicates per sample.

151 **Metatranscriptomics and RNA sequencing:**

152 Cell pellets were re-suspended in TRIzol reagent and subjected to three cycles of 1min bead-beating
153 (0.5mm silica/zirconia beads) followed by RNA extraction using the Direct-zol RNA Kit (Zymo research)
154 according to the manufactures' protocol. DNA was removed by TURBO DNase (Ambion) until no genomic
155 DNA was detected by PCR. The quality and integrity of the total RNA were checked on the Bioanalyzer
156 system (Agilent). Because RNA yield is low, only 6 samples containing the highest amount of RNA and best
157 RIM values (>6) were selected for RNA sequencing and meta-transcriptomic analysis (data not shown).
158 Ribosomal RNA depletion was performed using the Bacteria RiboZero kit (Illumina). From rRNA-depleted
159 RNA, directional libraries were prepared using the TruSeq Stranded mRNA Sample preparation kit
160 following the manufacturer's instructions (Illumina). Libraries were quantified on Bioanalyzer DNA chips
161 (Agilent) and Qubit® dsDNA HS Assay Kit (ThermoFisher). 150 bp paired read sequences were generated
162 on the Nextseq 500 (high output) sequencer according to manufacturer's instructions (Illumina). The
163 multiplexing level was 10 samples per lane. Reads were cleaned for low-quality and adapter sequences
164 using Cutadapt version 1.11.

165 The level of ribosomal RNAs (rRNAs) remained high in our environmental samples, even after both *in vitro*
166 rRNA depletion step and optimized RNA extraction methods (see above). We tackled these technical
167 shortcomings by including an *in-silico* rRNA depletion step to improve mRNA read assembly and
168 subsequent analysis (Supplementary Fig. 2 and Supplementary Tables 2 and 3). Ribosomal RNA reads
169 were filtered out by mapping on the Silva database with BWA-MEM v0.1.17 (default parameters) and
170 Samtools v1.9 (36). Then, unmapped reads (mRNA) were subjected to *de novo* assembly using SPADES
171 v3.13.1 (k-mer length 21). From 31% to 42% of trimmed reads coding for rRNA per sample were fast
172 assigned to bacterial families with Kraken [39] against the Silva SSU/LSU-Ref database (Release 132) [40].
173 27% to 31% of reads corresponded to not classifiable metagenomics sequences, related to microbial dark
174 matter [41]. 0.68% to 12% of reads were classifiable on the 16S rRNA Silva database. (Supplementary
175 Figure 6, Supplementary Table 3).

176 After sequencing, trimming and *in silico* ribosomal RNA depletion, we obtained 4.137.706 putative mRNA
177 reads (57.77 % of the initial sample) for the Hospital *in situ* biofilm, and 35.861.826 putative mRNA reads
178 (29.6% of the initial sample) for the Urban *in situ* biofilm, leading to a reasonable number of contigs to
179 analyse, with 866.221 and 2.379.394 contigs for the hospital and urban WW *in situ* biofilms, respectively
180 (Supplementary Table 2). For the hospital WW *in vitro* biofilms HL-1 and HL-2 (HL-2 = hospital WW *in vitro*
181 biofilm with ciprofloxacin added) 14.860.486 and 36.452.020 mRNA reads were obtained leading to

182 2.332.472 (HL-1) and 3.285.208 (HL-2) assembled contigs, respectively. For the urban WW *in vitro* biofilms
183 UL-1 and UL-2 (UL-2= urban WW *in vitro* biofilm + ciprofloxacin), 55.513.773 and 38.054.494 mRNA reads
184 were obtained leading to 3.483.745 and 2.684.771 assembled contigs, respectively (Supplementary Table
185 2 and 3).

186 **Metatranscriptomic analysis:**

187 Mapping the mRNA assemblies to specific reference databases enables to assess the expression levels of
188 functionally viable ARGs within biofilms.

189 A specialized database of the genes targeted by the high-throughput qPCR for the targeted resistome
190 analysis was built (accession numbers available in Supplementary Table 1) and used for mapping
191 assembled contigs with BWA-MEM v0.1.17 (with default parameters) and SAMtools v1.9. Then, the
192 transcriptome activity and abundance of ARGs was assessed by mapping reads on assembled contigs [42].
193 Reads were mapped against each ARG-like sequence identified from meta-transcriptomic assembly
194 contigs, using Bowtie2 v2.3.4.3 with default settings. The ARG-like sequences with > 100 mapped reads
195 were assigned to ARG transcripts.

196 To increase the chance of detecting active ARGs in hospital and urban wastewater biofilms, transcripts
197 coding for ARGs were searched against the CARD database (release 08/21/2019) by using the Resistance
198 Gene Identifier (RGI 3.1.0) retaining perfect and strict hits only [43]. The ARG-like sequences were
199 identified as ARG transcripts when their coverage was up to 80% with a minimum of 100 reads mapping.
200 The expression level of a particular ARG transcript in each sample was calculated by summing the number
201 of hits by ARG class (see list of categories in Supplementary table 3). In addition, we weighted the
202 identification with the mean of read coverage by ARG class.

203 In addition, we detected ARG-carrying MGEs in WW biofilms, namely the active resistance mobilome.
204 First, assembled contigs were mapped against the ACLAME database [44], using BWA and Samtools.
205 Subsequently, identified MGE-carrying contigs were again mapped against the CARD database to identify
206 ARG-carrying MGEs. If one MGE-carrying contig mapped to different ARGs, only hits with the best CIGAR
207 (extracted from the SAM file) were considered.

208 All steps described above were implanted in python-based modules, and all modules formed the
209 framework of the pipeline AROM, for ARg On Mobilome (Supplementary Figure 2). Lately, we added the
210 module get abundance to normalize gene expression levels according to the sample size (Gb), the length
211 of reads and the length of each ARG [45]. All changes to AROM

212 (https://github.com/sophiaachaibou/ARGmodules) are tracked in GitHub and the versions managed using
213 bioconda.

214 **Extracellular polymeric substances (EPS) staining for confocal scanning laser microscopy:**

215 The following stains were used to fluorescently label EPS components (polysaccharides, lipids, and
216 external DNA) and to assess live-dead ratios of different biofilm samples. Life-dead: Propidium Iodide (red;
217 0.5µM working solution) and SYTO-BC (green; Life technologies™; 5uM working solution). 500µl of each
218 fluorescent dye applied and allowed to incubate at ambient temperature in the dark for 30 min. Slides
219 were subsequently rinsed three times with phosphate buffered saline (PBS) and immediately analyzed by
220 CSLM. For the EPS components, biofilms were fixed in 3.7% formaldehyde solution (see above) prior to
221 EPS staining. For external DNA (eDNA) the combination of TOTO-1 (green) and SYTO-60 (red) (Life
222 technologies™) was used. Staining was performed as described by Okshevsky et *al.* [46], by using a final
223 working stock solution in PBS of TOTO-1 at 2µM and SYTO-60 at 10µM. Here, following three PBS washes,
224 slides kept at 4°C in the dark until CSLM analysis the same day. For polysaccharides (carbohydrate binding
225 proteins) and proteins a combination of Concanavalin A, tetramethylrhodamine conjugate (ConA; Thermo
226 Fischer Scientific) selectively binding to α-mannopyranosyl and α-glucopyranosyl residues (carbohydrates)
227 and Fluorescein isothiocyanate isomer I (FITC; Siegma Aldrich) selectively binding to proteins was used.
228 FITC working solution was concentrated at 200µg/ml. 500µl of 0.1M sodium bicarbonate buffer was added
229 to the biofilm slide prior to adding 500µl of FITC staining solution (2µg/ml) and incubated at RT in the dark
230 for 30 minutes. Afterwards the excess stain was removed by washing the biofilm slide gently with 1 x PBS
231 solution for three times. Subsequently 500µl of ConA staining solution (50µg/ml) was added to the slide
232 and incubated for 30 minutes at RT in the dark. Excess stain was removed by washing three times with 1x
233 PBS solution. Slides were stored at 4°C until CSLM analysis. For lipid and internal lipid droplet staining Nile
234 Red (0.1µg/ml) was used in combination with FITC (2µg/ml). Incubation and staining were performed as
235 described above by first applying 500µl of 0.1M sodium bicarbonate buffer, subsequently 500µl of FITC
236 working solution, incubation for 30 minutes at RT in the dark, washing with PBS for removal of excess FITC
237 staining and addition of 500µl of Nile Red working solution, incubation for 30 minutes at RT in the dark,
238 removal of excess dye by washing with PBS three times, and storing at 4°C until analysis by CSLM.

239

240 **Confocal scanning laser microscopy settings and analysis:**

241 Z stacking acquisitions were acquired with a confocal microscope (ZEISS LSM880) using a x20 and x100
242 magnification. Five Z stacks were performed per condition. The following settings were used to measure
243 the fluorescence from the samples: autofluorescence (λexc 405nm/λem 460nm), FITC (λexc 488nm/λem
244 525nm), tetramethylrhodamine (λexc 561nm/λem 580nm), Nile Red (λexc 641nm/λem 650nm), Syto60
245 (λexc 641nm/λem 678nm) and TOTO-1 (λexc 514nm/λem 533nm).

246 3D view analysis was performed with the Imaris software (Oxford Instrument) using acquisitions with the
247 x20 magnification. Surfaces were created using a manual thresholding. The quantitative analysis was
248 performed with the open-source software BiofilmQ (https://drescherlab.org/data/biofilmQ/) on the
249 acquisitions made with the x100 magnification. Each fluorescent z-stack was segmented using an
250 automatic thresholding (otsu algorithm) allowing object detection and measurements. We focused on the
251 relative abundance that is the measurement of the proportion of the biovolume occupied by each
252 component (i.e one staining). This biovolume must be understood as the total volume occupied by
253 staining(s) of interest. The relative abundance of the polysaccharides (stained by concanavalin A) and the
254 lipids (stained by nile red) were expressed as a percentage of the biovolume resulting from the merge
255 between concanavalin A OR fluorescein, and between nile red OR fluorescein respectively. eDNA relative
256 abundance was expressed as a percentage of the TOTO-1 staining (i.e eDNA) regarding the biovolume
257 resulting from the merge between TOTO-1 OR SYTO-60 stainings.

258 **Statistical analysis**

259 **Biofilm matrices**

260 To test for the effect of sample origin (hospital vs urban WW), environment (*in situ* vs *in vitro*) and addition
261 of ciprofloxacin on the composition of the biofilm matrices, the relative abundance of three features were
262 measured, the eDNA, lipid and polysaccharides. For each of these features three models were built. The
263 first type of model focused on data obtained without ciprofloxacin and analyzed for each measured
264 feature, the effect of the variables 'sample origin' and 'environment', as well as their interactions. The
265 second type of model focused on data obtained in the *in vitro* environment and analyzed for each of the
266 three measured features, the effect of the variables 'sample origin' and 'ciprofloxacin', as well as their
267 interactions. The last type of model is devised to perform a pairwise comparison of each sample, hence,
268 a different model was built for each pair of samples, with one explanatory variable and two levels,

corresponding to the sample ID. All these tests were based of the Randomization of Residuals in a Permutation Procedure implemented by the R package RRPP.

Pairwise comparison of the normalized abundance of the resistome data using the Tukey HSD test

To compare the relative abundances of genes classes between samples, for each class and biological replicate, we summed the normalized abundances of individual genes per class. Then for each gene class, we fitted the relative abundance with a log linear model with one explanatory variable, and one level for each sample. Finally, we applied pairwise comparisons of samples using the Tukey HSD test implemented by the multcomp R package and p-values were adjusted using the single step method [47].

Correlation of the normalized abundance for ARGs detected by qPCR and their likelihood to be expressed and detected by our meta-transcriptomic pipeline

To detect the threshold for normalized abundance values of genes measured by qPCR, below which meta-transcriptomic has a low chance of detecting the expression of the gene, we fitted a binomial generalized linear model (GLM) explaining the presence or absence of mapped reads (obtained for individual genes detected by our meta-transcriptomic pipeline) by the normalized abundance of the respective genes measured by qPCR. This allowed to obtain a cut-off value for normalized abundance determined by qPCR that is predicted to have a chance of being expressed and detected by our meta-transcriptomic pipeline. We also fitted a Poisson GLMM to the exact read maps for genes detected by our meta-transcriptomic pipeline, with the same explanatory variable as in the binomial GLM, and in addition, an observation level random effect, to account for overdispersion [48].

Pairwise comparison of biofilm communities, mobilome and resistome

For the six types of multivariate description of the biofilms, communities (family and genus levels), mobilome (plasmid and gene levels) and resistome (targeted and non-targeted), we compared each pair of samples by measuring the proportion of the Simpson's diversity that was between samples. Simpson's diversity measures the probability that two entities taken at random from the dataset are of the same type. It is calculated as $1 - \sum {f_i}^2$, where values of $f_.$ are the frequencies of the entities. To compute the proportion of this Simpson's diversity that is between a given pair of samples A and B, we computed the total diversity using the average of the frequencies of the two samples and the average diversity within the two sample:

$$D_{AB} = 1 - \frac{(1 - \sum {f_{iA}}^2) + (1 - \sum {f_{iB}}^2)/2}{1 - \sum \left((f_{iA} + f_{iB})/2 \right)^2}$$

298 This divergence index turns out to also be the formula of the between population fixation index (F_{ST}) used
299 in population genetics, using alleles frequencies [49].

300 Based on these pairwise dissimilarities, we built UPGMA trees (unweighted pair group method with
301 arithmetic mean). The stability of the trees was assessed by bootstrapping the individual genes and taxa.
302 To assess the significance of the divergence between samples we used the pair of samples with the lowest
303 divergence as a conservative reference. Specifically, we categorized bootstraps according to the pair of
304 samples with the lowest divergence, and then calculated the proportion of each category. Finally, we
305 assessed and tested the correlation between the dissimilarity matrices used to build the UPGMA trees
306 using some Mantel tests (R package ade4).

307 **Multivariate analysis for ARG detected on plasmids (mobilome)**

308 To analyze the association between the class of the ARGs of the mobilome and the WW origin of the
309 biofilm and their treatment (*in situ*, *in vitro*, with or without ciprofloxacin), we first performed a
310 correspondence analysis (CA; function 'dudi.coa' of the ade4 R package) analyzing the link between the
311 relative abundance of each ARG associated to a MGE. The significance of this association was tested
312 through a χ^2-test with a p-value based on 10^5 Monte Carlo simulations, and its effect size through the
313 Cramér's V statistic, a measure of the association between two categorical variables that varies from 0
314 (no association) to 1 (complete association). Then ARGs were grouped into gene classes, and the
315 association between gene classes and biofilm origin and treatment was investigated by applying between
316 class analysis (function 'bca' of the ade4 R package) to the CA. We refer to this overall analysis as to a
317 between correspondence analysis (bCA) which significance was assessed though a 10^5 permutation test.
318 This bCA recovered 33% of the total variation.

319

320 **Results**

321 **Effects of minimal selective concentrations (MSC) of ciprofloxacin, sample origin and**
322 **environment, on hospital and urban WW biofilms' extracellular polymeric substances (EPS)**

323 We first analyzed the global structure of the hospital and urban WW biofilms. The EPS (eDNA, lipids and
324 polysaccharides) were visualized by confocal scanning laser microscopy (CSLM). 3-D imaging (IMARIS) and
325 quantitative analysis (Biofilm Q) showed that the EPS significantly differ between their growth
326 environment, namely whether biofilms were grown *in situ* or, as reconstituted biofilms, *in vitro*. We
327 detected different relative abundance of eDNA (in both hospital and urban biofilms compared to their *in*
328 *vitro* counterparts), polysaccharides (for urban *in situ* vs *in vitro* + cip biofilms) and lipids (for hospital *in*
329 *situ* vs *in vitro* biofilms) (Figure 1 and 2, Supplementary Figure 4a and 4b, Supplementary Table 5). We also
330 detected significant differences in the relative abundance of EPS components dependent on the sample
331 origin, meaning between hospital and urban *in situ* WW biofilms, for eDNA and lipids (Figures 1 and 2,
332 Supplementary Figure 4a and 4b). The relative abundance of eDNA was higher for the hospital *in vitro*
333 biofilms compared to the urban *in vitro* WW biofilms. We also assessed the impact of adding ciprofloxacin
334 on the life-dead ratio and EPS components of the *in vitro* reconstituted hospital and urban WW biofilms.
335 A significant increase of dead cells was detected for the hospital *in vitro* biofilm after adding ciprofloxacin,
336 compared to its control (Supplementary Figure 3). The relative abundance of eDNA was significantly lower
337 in the hospital *in vitro* biofilm exposed to ciprofloxacin and significantly lower for polysaccharides in the
338 urban *in vitro* biofilm exposed to ciprofloxacin compared to their control.

339 Finally, we implemented statistical models based on random permutations testing for an overall effect of
340 the environment (*in situ* vs *in vitro*), the sample origin (hospital vs urban) and the effect of ciprofloxacin,
341 on the EPS components of these biofilms (Supplementary Table 5). We confirmed that i) the sample origin
342 (type of hospital vs urban WW) has a significant impact on the abundance of polysaccharides and lipids,
343 and eDNA ii) whether biofilms are grown *in situ* or *in vitro* has a significant impact on the relative

abundance of eDNA and iii) ciprofloxacin has a significant impact on the abundance of polysaccharides for both, hospital, and urban *in vitro* biofilms (Supplementary Table 5).

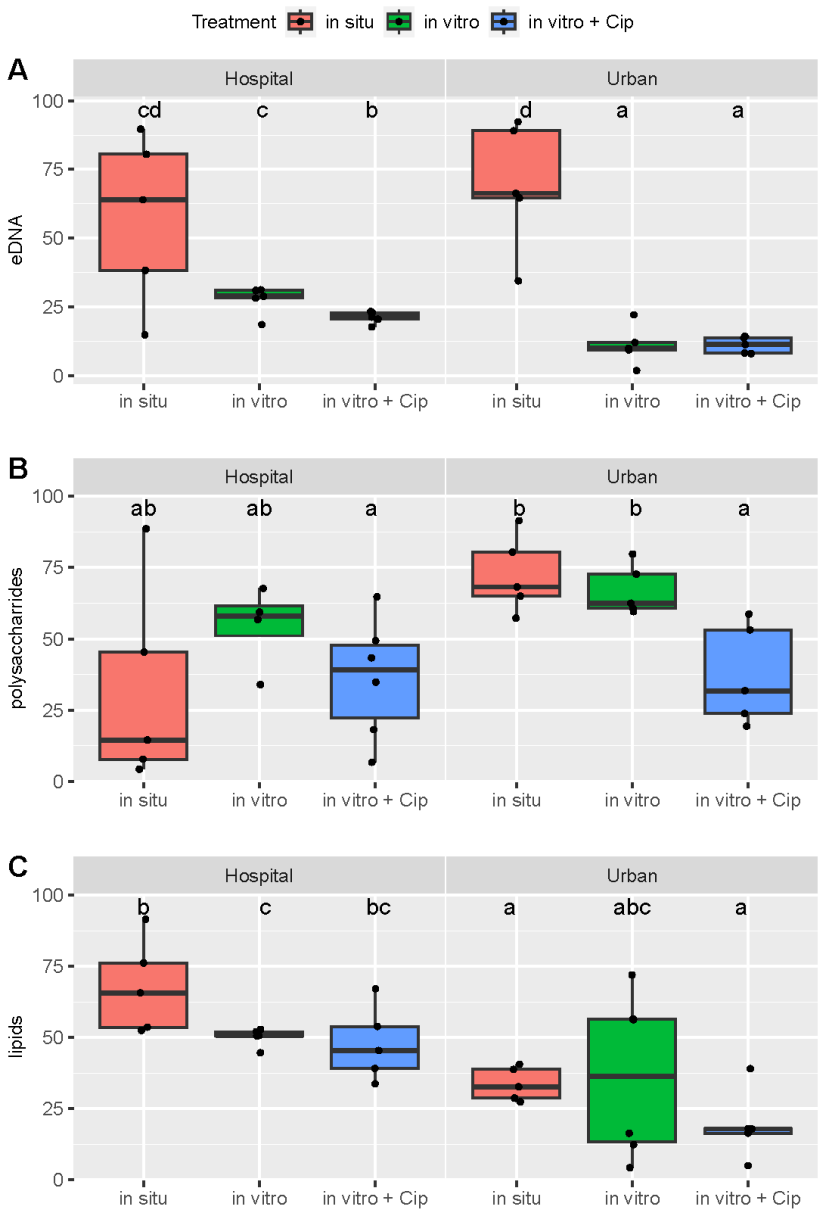

Figure 1: Relative abundance of eDNA (A), polysaccharides (B) and lipids (C) in the respective biofilms. Each EPS component was stained in a different biological replicate, and fluorescence was detected by 5 z-stack acquisitions for each biofilm sample with a 100-fold magnification for the respective biofilms. Quantitative image analysis was performed with Biofilm Q. Results of pairwise permutations tests are summarized using the compact letter display. Samples that do not share a letter in common are significantly different from each other. +Cip= *in vitro* biofilms were exposed after 3 days of initial biofilm formation with 1 µg/ml ciprofloxacin for 4 consecutive days and harvested after exposure of 4 hours on the final day.

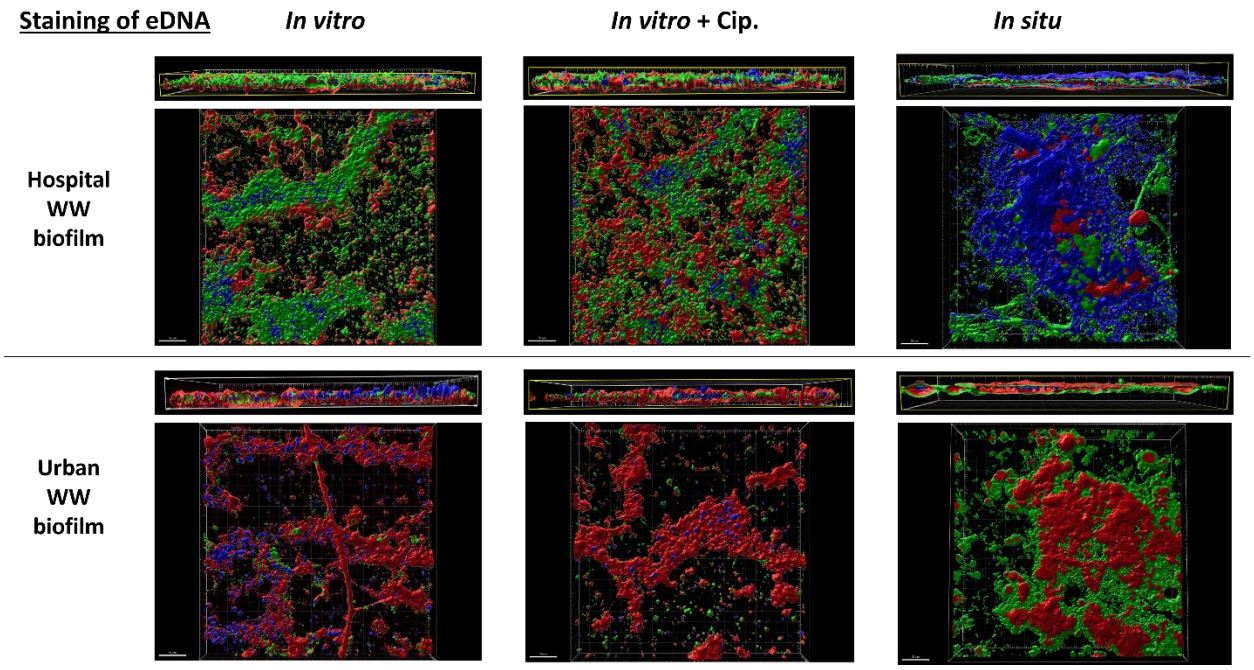

371

372 **Figure 2**: **3D imaging of eDNA (green) and total nucleic acids (red), for hospital and urban *in-situ* and *in-vitro***
373 **biofilms.** Autofluorescence for unknown compounds is in blue. +Cip= *in vitro* biofilms were exposed after 3 days of
374 initial biofilm formation with 1 µg/ml ciprofloxacin for 4 consecutive days and harvested after exposure of 4 hours
375 on the final day.

376

377 **The microbiota of hospital and urban WW *in situ* and *in vitro* biofilms**

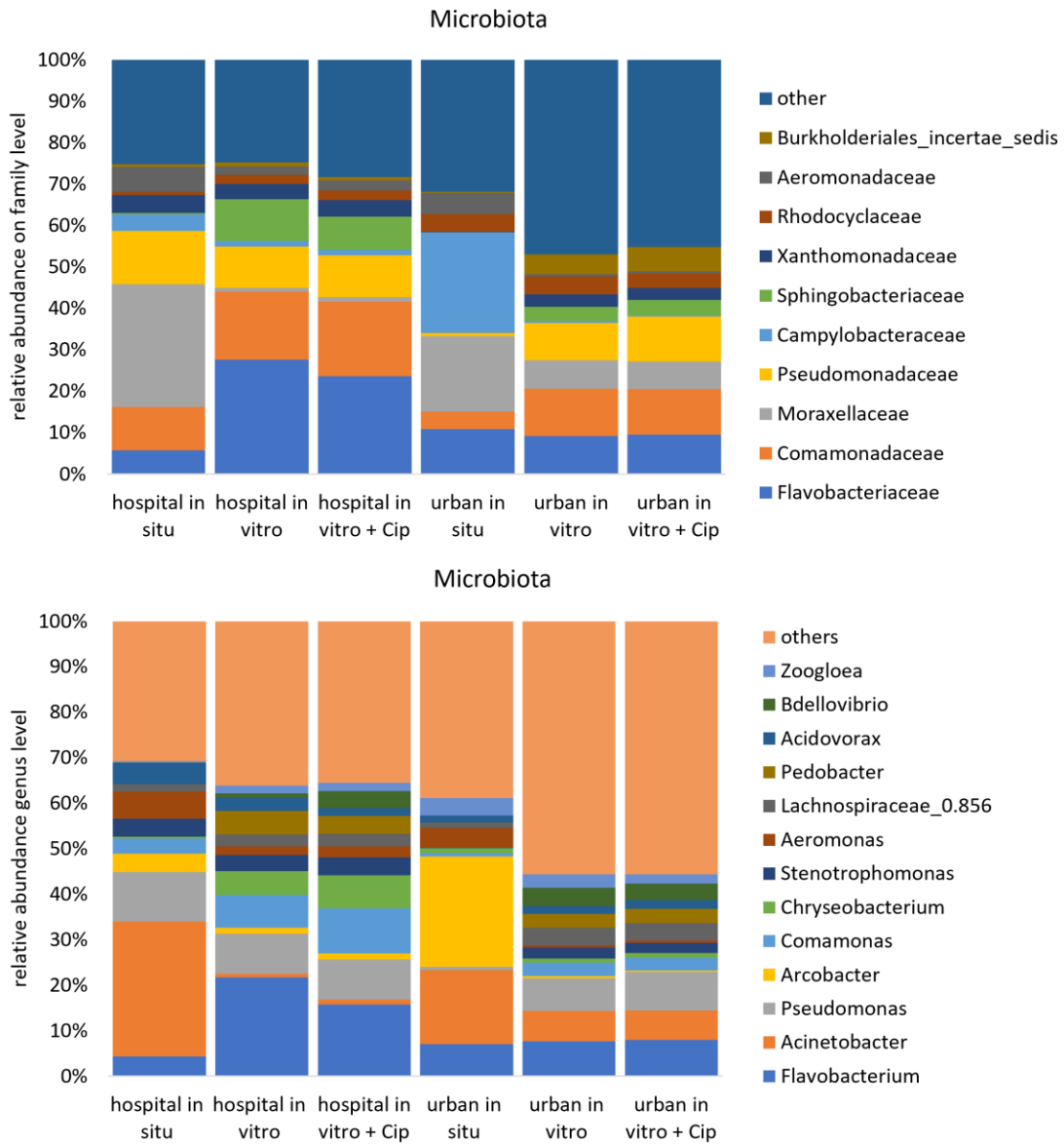

378

379 **Figure 3**: **Microbiota composition of hospital and urban wastewater *in situ* and *in vitro* biofilms based on**
380 **sequencing of the 16S rRNA gene.** Depicted are the top 10 taxa on order level and the top 12 on the genus level,
381 the remaining taxa are grouped into others. +Cip= *in vitro* biofilms were exposed after 3 days of initial biofilm
382 formation with 1µg/ml ciprofloxacin for 4 consecutive days and harvested after exposure of 4 hours on the final day
383 (D7).

384 The microbial compositions of WW biofilms were assessed using 16S rDNA sequencing. Strikingly and in
385 line with the phenotypic analysis of the biofilm structures, bacterial community profiles of hospital and
386 urban *in situ* biofilms were significantly different from their *in vitro* reconstituted counterparts
387 (Supplementary Figure 5 and Supplementary Table 6). The main genera in the *in situ* hospital WW biofilms

388 are Gram-negative pathogens such as *Pseudomonas*, *Acinetobacter* and *Aeromonas,* responsible for
389 infections in hospitalized patients [50–52] (Figure 3). *In situ* urban WW biofilms are dominated by different
390 genera than hospital WW biofilms, namely *Flavobacterium* and *Arcobacter* but share *Acinetobacter* with
391 hospital *in situ* biofilms. The genus *Arcobacter* is a common member of human WW systems and can rarely
392 act as animal and human pathogen [53,54]. It is more abundant in urban WW biofilms, compared to the
393 hospital WW environment. *Pseudomonas* is a dominant genus in both urban and hospital *in vitro* biofilms.
394 Surprisingly, *Acinetobacter* decreased in the *in vitro* biofilms compared to their *in situ* counterparts. The
395 addition of ciprofloxacin to the WW in our *in vitro* model did not change the proportional microbiota
396 composition for biofilms from urban WW. However, it had a weak but significant effect on the microbiota
397 composition of biofilms from hospital WW (percentage of the Simpson's diversity between this pair of
398 samples < 0.2%; Figure 3; Supplementary Figure 5). This suggests that exposure of already formed WW
399 biofilms with ciprofloxacin at MSC in our *in vitro* model has no effect, or only a minor effect, on the primary
400 bacterial ecosystems.

401 As described in methods, a relatively large proportion of the RNA reads from the metatranscriptomic RNA
402 sequencing approach of the biofilm communities were ribosomal RNA (rRNA) reads. The 16S rRNA reads
403 were filtered out by mapping on the Silva database, allowing for the assignment of a small proportion of
404 those reads (between 0.68% and 12%) on family level. Hence, this step allowed for additional analysis of
405 the "active microbiota" of these biofilms. Among the classifiable 16S rRNA reads from the
406 metatranscriptomic analysis (methods), we identified a large majority of *Enterobacteriaceae* in hospital
407 biofilms and a mix of *Flavobacteriaceae*, *Enterobacteriaceae*, *Streptococcaceae* and *Francisellaceae* in
408 urban *in situ* biofilm (Supplementary Figure 6 and Supplementary Table 3).

409

410

411

The targeted resistome and its expression in hospital and urban WW biofilms

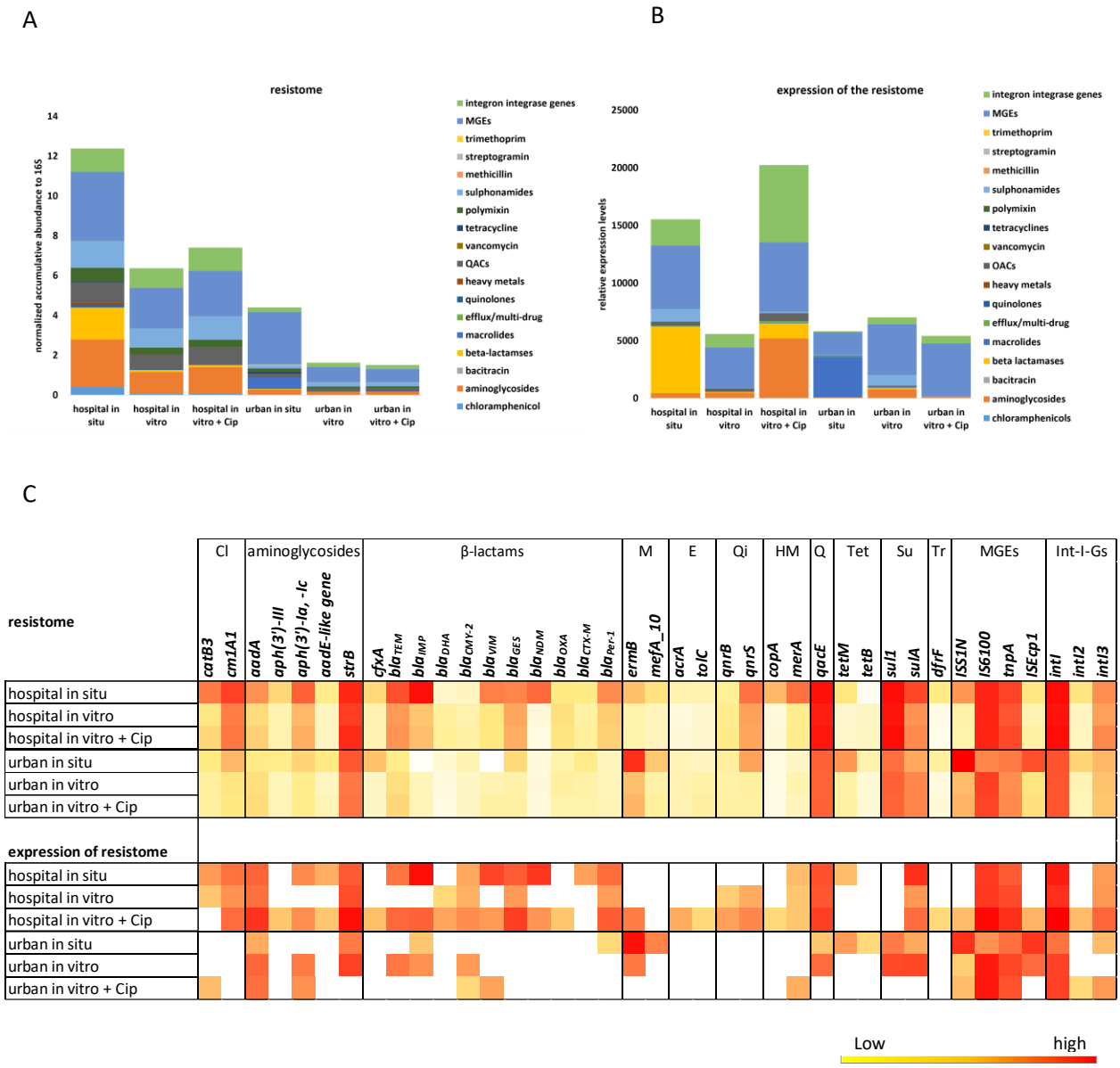

Figure 4: The targeted resistome and its expression in hospital and urban WW biofilms. On panel **A** and **B**, normalized abundance of the targeted resistome (A) and their expression (B) were grouped into gene classes and mobile genetic elements (MGEs) and integron integrase genes. **C**: Heatmap depicting the log2 of normalized abundance of individual genes (targeted resistome) and their normalized expression levels (exact counts of mapped reads for the respective genes) for the individual genes detected by metatranscriptomics. Data were log2 transformed for visualization purpose**.** +Ab= *in vitro* biofilms were exposed after 3 days of initial biofilm formation with 1µg/ml of the antibiotic ciprofloxacin for 4 consecutive days and harvested after exposure of 4 hours on the final day (D7). Cl= chloramphenicol; M= macrolides; E= efflux pumps/multi-drug resistance genes; Qi= quinolones; HM= heavy metals; Q= quaternary ammonium compounds (QACs); Tet= tetracyclines; MGEs= Mobile Genetic Elements. Int-I-Gs= integron integrase genes class I, II and III. +Cip= *in vitro* biofilms were exposed after 3 days of initial biofilm formation with 1 µg/ml ciprofloxacin for 4 consecutive days and harvested after exposure of 4 hours on the final day.

429 To assess the resistome in our samples, a targeted high-throughput qPCR approach, that detects and
430 quantifies 87 individual genes conferring resistance to clinically relevant antibiotics, quaternary
431 ammonium compounds (QACs), heavy metals, transposase genes (MGEs) and integron integrase genes,
432 also referred to as targeted resistome, was applied. At first, comparing the different environments in
433 which biofilms grew (*in situ* vs *in vitro*), we found that for the hospital WW biofilms, all gene classes had
434 a higher normalized abundance in *in situ* biofilm compared to the *in vitro* biofilms, except for
435 aminoglycosides, quinolones, QACs, sulphonamides, MGEs and integrons, which were not significantly
436 different (Figure 4 a and c, Supplementary Figure 7, and Supplementary Table 7). Performing the same
437 comparison for the urban WW *in situ* vs the *in* vitro biofilms, the normalized abundances of
438 chloramphenicol, macrolides, quinolones and MGEs, were significantly higher for the *in situ* biofilms,
439 whereas genes conferring resistance to heavy metals, vancomycin, and sulphonamides had significantly
440 lower normalized abundances in *in situ* urban WW biofilms. Then, comparing the different sampling origin
441 (hospital vs urban WW), the normalized abundance of the targeted resistome was highest in the *in situ*
442 hospital WW biofilms for all detected gene classes apart from macrolides, which were higher in the urban
443 *in situ* biofilm, while tetracyclines, quinolones and MGEs, were not significantly different in their
444 normalized abundance between the two *in situ* biofilm sampling origins (Supplementary Figure 7, and
445 Supplementary Table 7). Comparing the normalized abundance of detected gene classes for the hospital
446 *in vitro* biofilms vs the urban *in vitro* biofilms, it was higher in the hospital *in vitro* biofilms for most genes,
447 except for macrolides, vancomycin and genes encoding for multi-drug efflux pumps for which the
448 normalized abundance was higher in the urban *in vitro* biofilms; no significant difference was observed
449 for tetracyclines and heavy metal resistance genes.

450 Then, we analysed the metagenomic messenger RNA (mRNA) to provide information about the targeted
451 resistome actively being expressed in the *in situ* and *in vitro* hospital and urban WW biofilms. Overall, 39
452 of the 87 targeted genes by qPCR were expressed in at least one of the samples (Figure 4b and c).
453 Following the same comparison pattern, when first comparing the biofilm environments (*in situ* vs *in*
454 *vitro*), beta-lactam, chloramphenicol and sulphonamide resistance genes were 112, 5, and 47-fold higher
455 expressed in the hospital *in situ* biofilm vs *in vitro* biofilm, whereas macrolide resistance genes were 49-
456 fold higher expressed in the urban *in situ* biofilm compared to *in vitro* biofilm, while for all other gene
457 classes were gene expression could be detected, these detection levels were lower in the urban *in situ*
458 biofilm vs *in vitro* (Figure 4b and c, Supplementary Table 8 and Supplementary Figure 8). For the different
459 sample origins (hospital vs urban WW) of the studied biofilms, expression levels were higher for 7 gene
460 classes, from 5.5-fold higher for genes conferring resistance to aminoglycosides to 957-fold higher for

461 genes conferring resistance to beta-lactams, (Supplementary Table 8 and Supplementary Figure 8) for the
462 *in situ* hospital vs urban *in situ* WW biofilms.

463 We studied the impact of ciprofloxacin in the *in vitro* biofilm models. When looking at normalized
464 abundance of the targeted resistome in hospital and urban *in vitro* biofilms exposed to ciprofloxacin, no
465 differences could be detected, except for genes conferring resistance to macrolides in the hospital *in vitro*
466 biofilm exposed to ciprofloxacin compared to its control. (Supplementary Figure 7, and Supplementary
467 Table 7). Interestingly, we observed an enhanced expression of the targeted resistome (Figure 4b and c,
468 Supplementary Table 8 and Supplementary Figure 8) after ciprofloxacin addition in the hospital biofilm.
469 For example, expression of ARGs conferring resistance to beta-lactams was 26-fold higher and
470 aminoglycoside resistance genes were expressed 11-fold higher and represented the class of ARGs that
471 was most abundantly expressed proportionally within the hospital biofilm (Figure 4b and c,
472 Supplementary Table 8 and Supplementary Figure 8). Furthermore, ciprofloxacin enhanced expression (4-
473 fold) of the quinolone-resistance genes, *qnrB* and *qnrS* genes, and integron integrase genes (*IntI1* and
474 *IntI3*) by 6-fold and the grouped transposase genes by 1.7-fold compared to its control (Figure 4b and c,
475 Supplementary Table 8 and Supplementary Figure 8). When looking at the detected expression levels of
476 ARG classes in the urban *in vitro* biofilm exposed to ciprofloxacin, expression of ARGs was lower for all
477 detected gene classes apart from the integron integrase and aminoglycoside genes, were expression
478 slightly increased by 1.1 and 1.7-fold respectively, compared to its control (Figure 4b and c, Supplementary
479 Table 8 and Supplementary Figure 8). The *ISS1N* gene was specifically expressed in the *in situ* urban WW
480 biofilm.

481 Overall, these findings showed that 45% of the targeted resistome is expressed in the WW biofilms and
482 that the expression of ARGs and integron integrase genes in the *in vitro* hospital WW biofilm is enhanced
483 by the addition of ciprofloxacin. Interestingly, genes that were the most abundant in the targeted
484 resistome (qPCR) had a higher probability of being expressed and detected by metatranscriptomics. For
485 example at a threshold of 0.057 for the normalized abundance of genes in the targeted resistome the
486 probability of being expressed and detected by metatranscriptomics is 0.5 (Rho=0.77; Supplementary
487 Figure 10 and Supplementary Table 10).
488 Below this threshold, the detection of ARG expression could no longer be achieved, suggesting a lack of
489 transcripts. However, technical limitations such as the low sensitivity of meta-transcriptomics and/or the
490 detection of DNA from dead cells and eDNA by qPCR might also be possible explanations as to why not
491 more of the targeted genes could be detected by the metatranscriptomic approach [55–57].

492 **Assessing the expression of ARGs based on the CARD database**

493 To identify additional ARGs that were not included in our targeted resistome approach, mRNA reads of
494 our samples were mapped against the Comprehensive Antibiotic Resistance Database (CARD) that
495 archives thousands of gene sequences encoding resistance determinants to antimicrobial agents.

496 ARG expression was higher for *in situ* hospital WW biofilms compared to their *in vitro* counterpart (10.4%
497 for hospital *in situ* biofilm vs about 0.5% for *in vitro* of total mRNA reads in the respective samples
498 (Supplementary Table 1)). The detected expression levels of ARGs in the *in situ* urban WW biofilms was
499 lower compared to their *in vitro* counterpart (0.04% of mRNA reads for the urban *in situ* vs urban *in vitro*
500 0.4% biofilm). A tenfold higher expression level of ARGs was detected in the *in situ* hospital WW biofilm
501 (10.4 % of all mRNA reads coding for ARGs) compared to the urban WW *in situ* biofilm (0.04 % of mRNA
502 reads coding for ARGs) (Supplementary Table1). For the *in vitro* hospital biofilm exposed to ciprofloxacin,
503 expression level of ARGs was about 4.4-fold higher compared to the non- exposed one (2.4% vs 0.55% vs,
504 (Supplementary Table 1)). No difference in ARG expression level based on total ARG mRNA reads could
505 be observed between urban *in vitro* biofilms exposed or not to ciprofloxacin for the normalized data
506 (0.41% vs 0.37% of total mRNA reads mapping to ARGs, respectively, Supplementary Table 1).

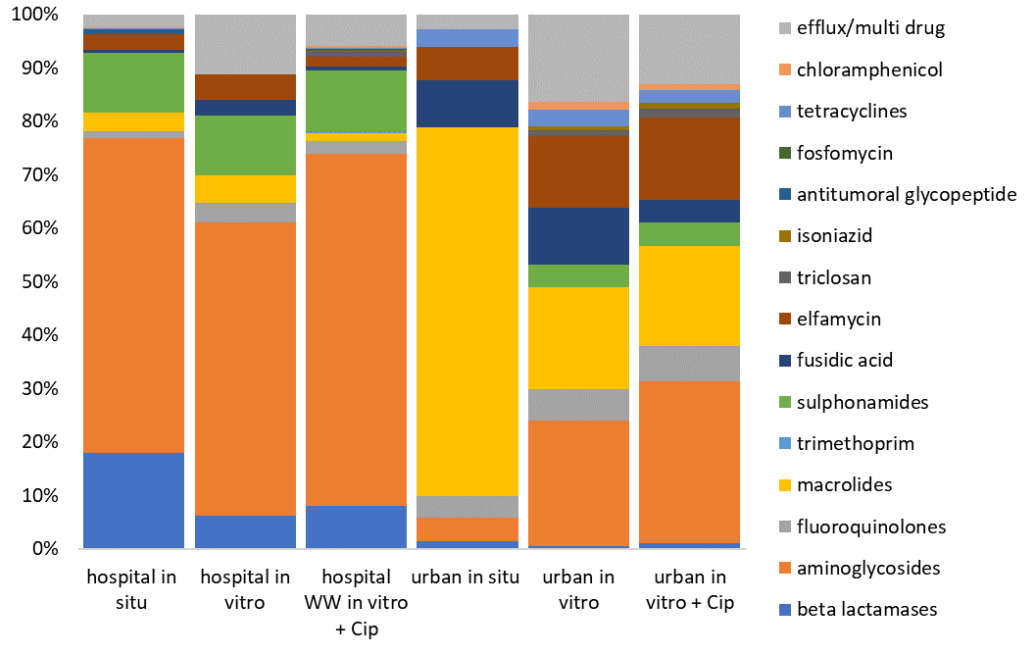

507

508 **Figure 5: ARG metatranscriptome based on the CARD database.** Mean numbers of mapped reads per
509 antimicrobial resistance gene were summed by ARG class and are displayed per sample.

510

511 In total we detected the expression of 70 individual resistance genes conferring resistance to 16 classes
512 of antibacterial drugs across all biofilm samples (Figure 5, Supplementary Tables 4 and 9). This approach
513 led to the detection of the expression of additional genes in hospital and urban WW biofilms that were
514 not detected by the targeted approach (Supplementary Table 4). For example, active beta-lactamase such
515 as *bla*^{RCP}, *bla*^{LCR}, *bla*^{FOX}, *bla*^{NPS}, four aminoglycoside-modifying enzymes (*aac(3)-Ib/aac(6')-Ib*, *aad*B,
516 *aph*(3''), *aph*(6)) and a macrolide phosphotransferase (MPH) were identified. Genes that confer resistance
517 to the antimicrobial classes fusidic acid, elfamycin, rifamycin and antitumoral glycopeptides were found
518 to be actively expressed in all the investigated samples. Genes that confer resistance to isoniazid and
519 triclosan were found to be expressed in the *in vitro* hospital biofilm exposed to ciprofloxacin, and in *in*
520 *vitro* urban WW biofilms in both conditions. The expression of an enterobacterial fosfomycin resistance
521 gene (*ptsI*) was detected in the *in vitro* hospital WW biofilm exposed to ciprofloxacin (Supplementary
522 Table 4). Furthermore, the expression of multidrug efflux pumps, specifically RND and MFS types, and the
523 expression of the *bla*^{OXA} beta-lactamases was detected in all the samples.

524 Overall the composition of the ARG metatranscriptome of the CARD resistome analysis correlated to the
525 targeted resistome analysis (Supplementary Figure 5, Supplementary Table 4 and 9). Comparing the
526 different environments for hospital biofilms (*in situ* vs *in vitro*), higher gene expression levels were
527 detected for the *in situ* hospital biofilm between 3.2-fold and 15.2-fold (macrolides and beta-lactamases
528 respectively). For the *in situ* vs *in vitro* urban biofilms, expression levels were lower for all detected ARG
529 classes, apart from macrolide ARGs, which were expressed at a higher level in urban *in situ* biofilm
530 (Supplementary Figure 9, Supplementary Table 4 and 9). For hospital *in situ* biofilm, six ARG classes had
531 between 1.8 and 81.2-fold higher expression levels (genes encoding resistance to fluoroquinolones and
532 aminoglycosides respectively) vs urban *in situ* biofilm. Comparing hospital *in vitro* biofilm exposed to
533 ciprofloxacin to its control, overall, increasing fold-change for seven ARG classes, between 3- and 7.5-fold
534 change for genes encoding for multi-drug efflux pumps and genes conferring resistance to beta-lactams,
535 respectively, was detected. Interestingly, 5 ARG classes, namely aminoglycosides, beta lactams,
536 quinolones, sulphonamides, and genes encoding for multi-drug efflux pumps, were detected to have
537 higher gene expression levels in both, the targeted and non-targeted resistome approach, for the hospital
538 *in vitro* biofilm exposed to ciprofloxacin compared to its control (Supplementary Figures 8 and 9,
539 Supplementary Table 4, 8 and 9). For the urban *in vitro* biofilm exposed to ciprofloxacin, expression levels
540 are lower, expect for genes encoding for beta-lactams were a slight increase (1.18-fold) could be detected
541 compared to its control (Supplementary Figure 9, Supplementary Table 4 and 9).

542 **The active resistance mobilome**

543 To study the expression of MGEs and more specifically MGEs associated with ARGs, assembled contigs
544 were mapped against the plasmid sequence collection v0.4 available at the ACLAME database [44].
545 Subsequently, plasmid associated contigs identified by this approach were mapped back to the CARD
546 database to identify specifically plasmids that carry ARGs. These ARG associated plasmids are referred to
547 as the "active resistance mobilome" in the respective samples.

548 Global expression of plasmids was very low in all the samples studied (0.48% of all assembled contigs for
549 hospital *in situ* biofilm and 0.14% for urban *in situ* biofilm (Supplementary Table 1)). In total, we counted
550 respectively 115 and 66 plasmid-ARG associated contigs for the hospital and urban *in situ* biofilms and
551 identified a diverse range of expressed plasmids (71 individual plasmids identified across all samples)
552 expressing a diverse range of ARGs that could be grouped into 10 classes conferring resistance to
553 antimicrobials, quaternary ammonium compounds and heavy metals. The highest expression level for the
554 active resistance mobilome was observed in the *in vitro* hospital biofilm exposed to ciprofloxacin
555 (Supplementary Figure 11).

556 55 different plasmids carrying a broad range of ARGs were identified as the active resistance mobilome
557 across all hospital WW biofilm samples. These plasmids were mainly resistance plasmids found in Gram-
558 negative pathogens such as the *bla-$_{VIM7}$* carrying plasmid *pmATVIM-7* first identified in *P. aeruginosa* [50];
559 the IncP-6 plasmid *Rms149,* a small resistant plasmid associated with *P. aeruginosa* [58] (detected only in
560 hospital *in situ* biofilm); several small resistance plasmids (e.g. *pKMA757, pARD3079, pKMA202,* and
561 *pKMA5)* associated with *Actinobacilli* [59] and plasmid families representing the groups IncP, F, N and Q
562 (Supplementary Figure 11). They primarily expressed aminoglycoside, sulphonamide, chloramphenicol,
563 and beta-lactam resistance genes (Supplementary Figure 11, Figure 6). 14 plasmids were detected in all
564 hospital WW biofilm samples, and 7 additional plasmids were only shared between the *in situ* hospital
565 WW biofilms and the *in vitro* hospital WW biofilm exposed to ciprofloxacin (Supplementary Figure 11).
566 Interestingly, 22 plasmids, carrying between 1 and 5 ARGs, were only identified in the *in vitro* hospital
567 WW biofilm exposed to ciprofloxacin (Supplementary Figure 11).

568 14 plasmids were unique for urban WW biofilm samples (*in situ* and *in vitro*). These plasmids mainly
569 carried macrolide and tetracycline resistance genes found in Gram-positive bacteria, such as Lactobacilli
570 (56). In addition, the *Enterococcus faecium* and *faecalis* plasmids *pRUM* and *pTEF1* were identified as
571 expressing both the macrolide resistance gene *ermB* [60–62] (Supplementary Figure 11). The broad host

572 range IncP-1 plasmid pKJK5 was also detected, expressing an aminoglycoside (*aadA6*) and a sulphonamide
573 (*sul1*) resistance gene [63,64]. One Gram-negative multidrug resistance plasmid *pJR1* [65] was detected,
574 carrying the chloramphenicol resistance gene *catB2* and the tetracycline resistance gene *tet(G)*
575 (Supplementary Figure 11). Fifteen plasmids were uniquely identified in the *in situ* urban WW biofilm and
576 not in its *in vitro* counterpart. Five of these plasmids were also detected in the hospital WW biofilms
577 expressing different ARGs (e.g. *pJHCMW1* and *R46*), whereas they only carried a single ARG when detected
578 in the *in situ* urban biofilm (Supplementary Figure 11).

579 In the hospital WW biofilms, many plasmids were identified to carry multiple resistance genes (up to 5
580 ARGs carried on one MGE contig, Supplementary Figure 11). These genes mainly encoded resistance to
581 aminoglycosides, beta-lactams, sulphonamides, chloramphenicol, and quaternary ammonium
582 compounds (Figure 6, Supplementary Figure 11). For the urban WW biofilms, MGEs that express multiple
583 resistance genes were also identified, but with less ARGs associated (maximum three ARGs on one plasmid
584 in the *in situ* urban WW biofilm) (Supplementary Figure 11). The ARGs mainly detected in the active
585 resistance mobilome of urban WW biofilms were macrolide, tetracyclines and multi-drug efflux pumps
586 (Figure 6, Supplementary Figure 11). Contrary to what is observed for the effect of ciprofloxacin on the
587 active resistance mobilome of the *in vitro* hospital biofilm, less MGE-ARG associated contigs were
588 identified, and a much lower diversity of ARGs were expressed in the *in vitro* urban biofilm exposed to
589 ciprofloxacin (mainly macrolide resistance genes) (Supplementary Figure 11, Figure 6).

590 Overall, correspondence analysis (CA) of our mobilome data, revealed a prominent association between
591 the ARGs present on plasmids and their biofilm origin (Cramér's V statistic = 0.604; χ^2-test *p*-value < 0.001;
592 Supplementary Figure 12). To assess if this association was also observed at the level of the ARGs classes,
593 we applied a between CA (bCA). This recovered 33% of the total association between biofilm origin and
594 the ARGs composition of the mobilome (*p*-value=0.026; Figure 6).

595

596

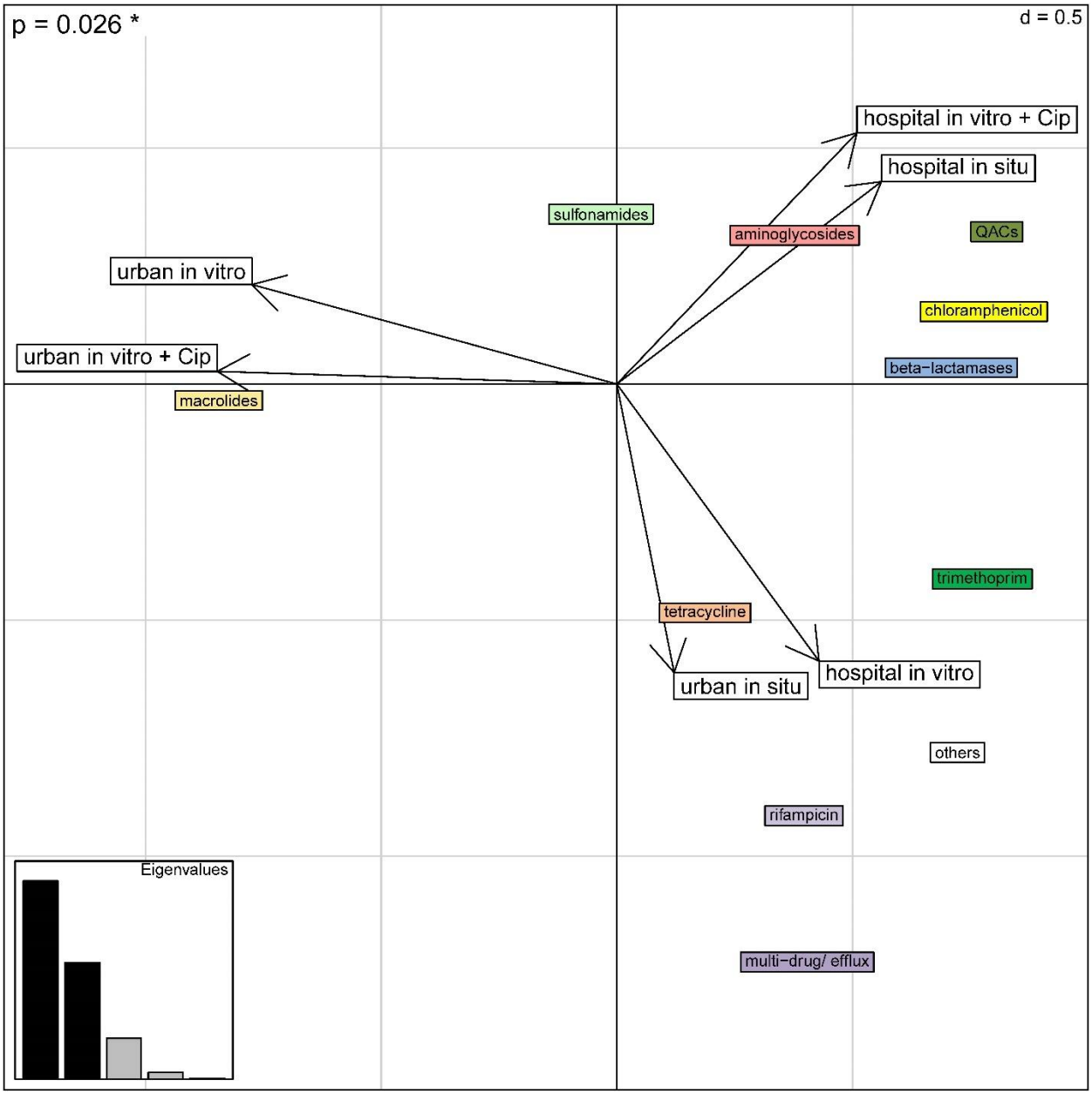

Figure 6: Between correspondence analysis (bCA) assessing the association between the type of ARGs classes present on plasmids, in terms of ARG class abundance (numbers of contigs) and the biofilm origin.

601 **Discussion**

602 The goal of this study was to develop a comprehensive experimental approach to assess WW biofilms as
603 putative hotspots for actual transfer of ARGs via MGEs within these communities using metagenomic
604 approaches. We furthermore wanted to quantify and visualize the EPS components of these biofilms, due
605 to the proposed role of the EPS in horizontal gene transfer within biofilms, as well as their relevance for
606 biofilms to tolerate antibiotics and exogeneous stressors [29,31,66–68].

607 Here we introduced a method by confocal laser scanning microscopy (CLSM) to visualize and quantify the
608 EPS of hospital and urban WW biofilms allowing to study EPS components in these biofilms over time and
609 under different anthropogenic constraints. We showed that i) the EPS components investigated are
610 differentially abundant dependent on their growth environment (*in* situ and *in vitro*) and their sampling
611 origin (hospital vs urban WW) and ii) ciprofloxacin at MSC impacted the quantity of the measured EPS
612 components. The decrease in the quantity of polysaccharides in the urban and in hospital *in vitro* biofilms,
613 and for eDNA in the hospital *in vitro* biofilm, due to the presence of ciprofloxacin might be linked to a
614 regulatory response of the biofilm community. Indeed, it has been shown that exogeneous stress in multi-
615 species biofilms leads to decreased EPS production [69]. *In vitro* eDNA was proportionally more abundant
616 in hospital WW biofilms compared to urban WW biofilms, which could be linked to higher amounts of
617 surfactants, antibiotics, and other pharmaceutical and chemical pollution in hospital WW [7] that in turn
618 may enhance bacterial lysis and active eDNA secretion in those biofilms [70]. eDNA is known to promote
619 tolerance to antimicrobial agents in biofilms by inhibiting the diffusion of cationic molecules [71] and by
620 increasing the resistance to aminoglycosides in *Pseudomonas aeruginosa* biofilms [72,73]. It has also been
621 shown that eDNA is involved in transfer of the ARG *tetM* by the conjugative transposon Tn916 [68],
622 through transformation. Transformation is suspected to be an important mechanism for gene transfer
623 between bacterial communities in biofilms [68]. We showed that the microbiota of hospital and urban
624 WW biofilms is distinct, which is likely correlated to the different organization and relative abundances
625 detected for the EPS in the two WW biofilm niches, as shown by our analysis (Supplementary Figure 5 and
626 Supplementary Table 6). The significant increase of dead cells observed for the *in vitro* hospital WW
627 biofilm exposed to ciprofloxacin could be linked to the predominant Gram-negative genera in hospital
628 WW biofilms (Figure 3), which are highly susceptible to ciprofloxacin.

629 By implementing a meta-transcriptomic approach, at first, we wanted to assess the basal differential
630 expression levels of mobile genetic elements (MGEs) associated with ARGs as a proxy for actual transfer
631 of ARGs within hospital and urban WW biofilms. Second, we wanted to compare these levels to *in vitro*

632 reconstituted biofilms and third, we wanted to see whether these "basal" expression levels do change in
633 response to a single antibiotic added to the WW environment. We showed that a) basal ARG and MGEs
634 expression levels are higher in *in situ* than *in vitro* WW hospital biofilms; b) expression levels of ARGs and
635 MGEs increase upon adding a minimal selective concentration (MSC) of ciprofloxacin to the *in vitro*
636 hospital WW biofilm environment and c) that expression of plasmids carrying specific ARG classes and
637 multiple ARGs at the same time, is associated with the biofilm origin (Figure 6). We were able to detect a
638 broad range of plasmids that were uniquely detected in either, hospital or urban WW biofilms.
639 Interestingly, plasmids detected in both, hospital and urban *in situ* and *in vitro* biofilms, carried different
640 types and quantities of ARGs (Supplementary Figure 9), suggesting that the plasmids cargo (content of
641 ARGs) is adapted to its environment. Hence, we showed that the nature of ARGs present on plasmids is
642 correlated to the biofilm environment and origin.

643 Interestingly, the reconstituted *in vitro* hospital and urban WW biofilms were more like each other
644 concerning their microbiota composition than their natural (*in situ*) biofilm counterparts, which was not
645 the case for the resistome, resistome expression nor active resistance mobilome. This surprising result
646 suggests that the *in vitro* laboratory conditions have a larger impact on the biofilm community structure
647 than the WW in which they developed. This questions the ability of our experimental set-up to implement
648 microcosms in the laboratory to mimic the natural environment. Further optimization of the *in vitro* model
649 is needed, which could be achieved for example by more frequent refreshment of the WW alimentation
650 in the *in vitro* system, or better control of the oxygen levels.

651 Among the classifiable rRNA reads from the metatranscriptomic analysis we identified a large majority of
652 *Enterobacteriaceae* in the hospital biofilms, and a mix of *Flavobacteriaceae*, *Enterobacteriaceae,*
653 *Streptococaceae* and *Francisellaceae* in the urban *in situ* biofilm (Supplementary Figure 6 and
654 Supplementary Table 2). The fact that these rRNA reads were obtained from the RNA sequencing run may
655 indicate that these families were highly "active" in these biofilms although not highly abundant based on
656 16S rDNA sequencing (Figure 3). The highly active proportion of *Enterobacteriaceae* in hospital *in situ* and
657 *in vitro* biofilms might indeed explain the higher expression levels and the types of MGEs and ARGs
658 detected in these samples, and their response to antibiotic stress. This further highlights the need to study
659 the 'active biofilm community' and might point towards the fact that the key players for accumulation
660 and transfer of ARGs and MGEs in highly anthropized sites such as WW are indeed human-gut associated
661 bacteria.

662 In a recent study, the Plascad tool was designed for plasmid classification, AMR gene annotation, and
663 plasmid visualization [74] and they showed that: i) most plasmid-borne ARGs, including those localized on
664 class-1 integrons, are enriched in conjugative plasmids in their datasets, and ii) transfer between AMR
665 plasmids and bacterial chromosomes was mediated by insertion sequences, mainly those belonging to
666 the IS6 family, IS26 and IS6100 [74]. We have shown previously that IS26 and IS6100 were both abundant
667 in WW [7] and in this study we show that IS6100 is highly expressed in hospital WW biofilms. IS26 is
668 frequently detected in plasmids of clinical importance associated with antibiotic resistance genes.
669 Furthermore, IS26 has also been associated with the expression of antibiotic resistance genes [75]. Finally,
670 the distinct plasmid profiles (Figure 6 and Supplementary Figure 11) and their specific ARG expression
671 profiles for hospital and urban WW biofilms point towards a strong environmental selection pressure
672 shaping the active resistance mobilome.

673 Here we provide an approach to comprehensively study multi-species biofilms that form in naturally as
674 well as highly anthropized environments such as WW. We show that hospital and urban wastewaters
675 shape the structure and active resistome of environmental biofilms, and we confirmed that hospital WW
676 is an important hot spot for the dissemination and selection of AMR. Hence, we propose that studying
677 hospital WW biofilms may present an ideal model to further unravel the complex correlation between
678 pollution and AMR selection and the structural, ecological, functional, and genetic organization of multi-
679 species biofilms as antibiotic resistance factories. Finally, our results highlight that for all studied biofilm
680 samples, resistome and mobilome significantly depended on their environment (*in vitro* vs *in situ*) and
681 origin (WW).

682

683

Data availability

16S rRNA sequence data are available at the European Nucleotide Archive (ENA) under the accession numbers ERS14475391-8. RNA sequencing data (metatranscriptomic data) will be available at the NCBI under project number PRJNA930611. All other important raw data needed to reconstruct the findings of our study are made available in the supplementary material.

Funding

E. Buelow has received funding from the European Union's Horizon 2020 research and innovation program under the Marie Skłodowska-Curie grant agreement RESOLVE 707999-standard EF.

Declaration of competing interest

The authors declare that they have no known competing financial interests or personal relationships that could have appeared to influence the work reported in this paper.

697 References

698 1. Balcazar JL, Subirats J, Borrego CM. The role of biofilms as environmental reservoirs of antibiotic
699 resistance. FrontMicrobiol. 2015;6:1216.

700 2. Hennequin C, Aumeran C, Robin F, Traore O, Forestier C. Antibiotic resistance and plasmid transfer
701 capacity in biofilm formed with a CTX-M-15-producing *Klebsiella pneumoniae* isolate.
702 JAntimicrobChemother. 2012;67:2123–30.

703 3. Ferreira C, Veldhoen M. Host and microbes date exclusively. Cell. 2012;149:1428–30.

704 4. Abe K, Nomura N, Suzuki S. Biofilms: hot spots of horizontal gene transfer (HGT) in aquatic
705 environments, with a focus on a new HGT mechanism. FEMS Microbiology Ecology. 2020;96. Available
706 from: https://doi.org/10.1093/femsec/fiaa031

707 5. Allen HK, Donato J, Wang HH, Cloud-Hansen KA, Davies J, Handelsman J. Call of the wild: antibiotic
708 resistance genes in natural environments. NatRevMicrobiol. 2010;8:251–9.

709 6. Flandroy L, Poutahidis T, Berg G, Clarke G, Dao MC, Decaestecker E, et al. The impact of human
710 activities and lifestyles on the interlinked microbiota and health of humans and of ecosystems. SciTotal
711 Environ. 2018;627:1018–38.

712 7. Buelow E, Rico A, Gaschet M, Lourenço J, Kennedy SP, Wiest L, et al. Hospital discharges in urban
713 sanitation systems: Long-term monitoring of wastewater resistome and microbiota in relationship to
714 their eco-exposome. Water Research X. 2020;7:100045.

715 8. Harris S, Morris C, Morris D, Cormican M, Cummins E. The effect of hospital effluent on antimicrobial
716 resistant *E. coli* within a municipal wastewater system. EnvironSciProcessImpacts. 2013;15:617–22.

717 9. Jia A, Wan Y, Xiao Y, Hu J. Occurrence and fate of quinolone and fluoroquinolone antibiotics in a
718 municipal sewage treatment plant. Water Research. 2012;46:387–94.

719 10. Hayes A, May Murray L, Catherine Stanton I, Zhang L, Snape J, Hugo Gaze W, et al. Predicting
720 selection for antimicrobial resistance in UK wastewater and aquatic environments: Ciprofloxacin poses a
721 significant risk. Environment International. 2022;169:107488.

722 11. Kim D, Nguyen LN, Oh S. Ecological impact of the antibiotic ciprofloxacin on microbial community of
723 aerobic activated sludge. Environ Geochem Health. 2020;42:1531–41.

724 12. Nakata H, Kannan K, Jones PD, Giesy JP. Determination of fluoroquinolone antibiotics in wastewater
725 effluents by liquid chromatography–mass spectrometry and fluorescence detection. Chemosphere.
726 2005;58:759–66.

727 13. Beaber JW, Hochhut B, Waldor MK. SOS response promotes horizontal dissemination of antibiotic
728 resistance genes. Nature. Nature Publishing Group; 2004;427:72–4.

729 14. Guerin É, Cambray G, Sanchez-Alberola N, Campoy S, Erill I, Re SD, et al. The SOS Response Controls
730 Integron Recombination. Science. American Association for the Advancement of Science;
731 2009;324:1034–1034.

732 15. Hu Y, Yang X, Qin J, Lu N, Cheng G, Wu N, et al. Metagenome-wide analysis of antibiotic resistance
733 genes in a large cohort of human gut microbiota. NatCommun. 2013;4:2151.

734 16. Forslund K, Sunagawa S, Coelho LP, Bork P. Metagenomic insights into the human gut resistome and
735 the forces that shape it. Bioessays. 2014;36:316–29.

736 17. Sommer MO, Church GM, Dantas G. The human microbiome harbors a diverse reservoir of antibiotic
737 resistance genes. Virulence. 2010;1:299–303.

738 18. Karkman A, Parnanen K, Larsson DGJ. Fecal pollution can explain antibiotic resistance gene
739 abundances in anthropogenically impacted environments. NatCommun. 2019;10:80-018-07992–3.

740 19. Pehrsson EC, Forsberg KJ, Gibson MK, Ahmadi S, Dantas G. Novel resistance functions uncovered
741 using functional metagenomic investigations of resistance reservoirs. FrontMicrobiol. 2013;4:145.

742 20. Singer AC, Shaw H, Rhodes V, Hart A. Review of Antimicrobial Resistance in the Environment and Its
743 Relevance to Environmental Regulators. FrontMicrobiol. 2016;7:1728.

744 21. McInnes RS, uz-Zaman MH, Alam IT, Ho SFS, Moran RA, Clemens JD, et al. Metagenome-Wide
745 Analysis of Rural and Urban Surface Waters and Sediments in Bangladesh Identifies Human Waste as a
746 Driver of Antibiotic Resistance. mSystems. American Society for Microbiology; 2021;6:e00137-21.

747 22. Manaia CM, Rocha J, Scaccia N, Marano R, Radu E, Biancullo F, et al. Antibiotic resistance in
748 wastewater treatment plants: Tackling the black box. EnvironInt. 2018;115:312–24.

749 23. Rizzo L, Manaia C, Merlin C, Schwartz T, Dagot C, Ploy MC, et al. Urban wastewater treatment plants
750 as hotspots for antibiotic resistant bacteria and genes spread into the environment: a review. SciTotal
751 Environ. 2013;447:345–60.

752 24. Haenni M, Dagot C, Chesneau O, Bibbal D, Labanowski J, Vialette M, et al. Environmental
753 contamination in a high-income country (France) by antibiotics, antibiotic-resistant bacteria, and
754 antibiotic resistance genes: Status and possible causes. Environ Int. 2022;159:107047.

755 25. Luo Y-H, Lai YS, Zheng C, Ilhan ZE, Ontiveros-Valencia A, Long X, et al. Increased expression of
756 antibiotic-resistance genes in biofilm communities upon exposure to cetyltrimethylammonium bromide
757 (CTAB) and other stress conditions. Science of The Total Environment. 2021;765:144264.

758 26. Proia L, von Schiller D, Sànchez-Melsió A, Sabater S, Borrego CM, Rodríguez-Mozaz S, et al.
759 Occurrence and persistence of antibiotic resistance genes in river biofilms after wastewater inputs in
760 small rivers. Environmental Pollution. 2016;210:121–8.

761 27. Flemming H-C, Wuertz S. Bacteria and archaea on Earth and their abundance in biofilms. Nat Rev
762 Microbiol. 2019;17:247–60.

763 28. Ratajczak M, Kaminska D, Dlugaszewska J, Gajecka M. Antibiotic Resistance, Biofilm Formation, and
764 Presence of Genes Encoding Virulence Factors in Strains Isolated from the Pharmaceutical Production
765 Environment. Pathogens. Multidisciplinary Digital Publishing Institute; 2021;10:130.

766 29. Flemming HC, Wingender J. The biofilm matrix. NatRevMicrobiol. 2010;8:623–33.

767 30. Xiao J, Koo H. Structural organization and dynamics of exopolysaccharide matrix and microcolonies
768 formation by Streptococcus mutans in biofilms. JApplMicrobiol. 2010;108:2103–13.

769 31. Soares A, Roussel V, Pestel-Caron M, Barreau M, Caron F, Bouffartigues E, et al. Understanding
770 Ciprofloxacin Failure in *Pseudomonas aeruginosa* Biofilm: Persister Cells Survive Matrix Disruption. Front
771 Microbiol. 2019;10:2603.

772 32. Buelow E, Bayjanov JR, Majoor E, Willems RJL, Bonten MJM, Schmitt H, et al. Limited influence of
773 hospital wastewater on the microbiome and resistome of wastewater in a community sewerage system.
774 FEMS MicrobiolEcol. 2018;

775 33. Chonova T, Lecomte V, Bertrand-Krajewski JL, Bouchez A, Labanowski J, Dagot C, et al. The SIPIBEL
776 project: treatment of hospital and urban wastewater in a conventional urban wastewater treatment
777 plant. EnvironSciPollutResInt. 2018;25:9197–206.

778 34. Bengtsson-Palme J, Larsson DG. Concentrations of antibiotics predicted to select for resistant
779 bacteria: Proposed limits for environmental regulation. EnvironInt. 2016;86:140–9.

780 35. Buelow E, Bello Gonzalez TDJ, Fuentes S, de Steenhuijsen Piters WAA, Lahti L, Bayjanov JR, et al.
781 Comparative gut microbiota and resistome profiling of intensive care patients receiving selective
782 digestive tract decontamination and healthy subjects. Microbiome. 2017;5:88-017-0309-z.

783 36. Langsrud S, Sundheim G, Holck AL. Cross-resistance to antibiotics of Escherichia coli adapted to
784 benzalkonium chloride or exposed to stress-inducers. JApplMicrobiol. 2004;96:201–8.

785 37. Buffet-Bataillon S, Tattevin P, Bonnaure-Mallet M, Jolivet-Gougeon A. Emergence of resistance to
786 antibacterial agents: the role of quaternary ammonium compounds--a critical review.
787 IntJAntimicrobAgents. 2012;39:381–9.

788 38. Gillings MR, Gaze WH, Pruden A, Smalla K, Tiedje JM, Zhu YG. Using the class 1 integron-integrase
789 gene as a proxy for anthropogenic pollution. ISME J. 2015;9:1269–79.

790 39. Wood DE, Salzberg SL. Kraken: ultrafast metagenomic sequence classification using exact
791 alignments. Genome Biology. 2014;15:R46.

792 40. Pruesse E, Quast C, Knittel K, Fuchs BM, Ludwig W, Peplies J, et al. SILVA: a comprehensive online
793 resource for quality checked and aligned ribosomal RNA sequence data compatible with ARB. Nucleic
794 Acids Res. 2007;35:7188–96.

795 41. Solden L, Lloyd K, Wrighton K. The bright side of microbial dark matter: lessons learned from the
796 uncultivated majority. Curr Opin Microbiol. 2016;31:217–26.

797 42. Evaluation of metatranscriptomic protocols and application to the study of freshwater microbial
798 communities - Tsementzi - 2014 - Environmental Microbiology Reports: /doi/abs/10.1111/1758-
799 2229.12180

800 43. Alcock BP, Raphenya AR, Lau TTY, Tsang KK, Bouchard M, Edalatmand A, et al. CARD 2020: antibiotic
801 resistome surveillance with the comprehensive antibiotic resistance database. Nucleic Acids Res.
802 2020;48:D517–25.

803 44. Leplae R, Lima-Mendez G, Toussaint A. ACLAME: a CLAssification of Mobile genetic Elements, update
804 2010. Nucleic Acids Res. 2010;38:D57-61.

805 45. Liu Z, Klümper U, Liu Y, Yang Y, Wei Q, Lin J-G, et al. Metagenomic and metatranscriptomic analyses
806 reveal activity and hosts of antibiotic resistance genes in activated sludge. Environ Int. 2019;129:208–20.

807 46. Okshevsky M, Meyer RL. Evaluation of fluorescent stains for visualizing extracellular DNA in biofilms.
808 Journal of Microbiological Methods. 2014;105:102–4.

809 47. Hothorn T, Bretz F, Westfall P. Simultaneous inference in general parametric models. Biom J.
810 2008;50:346–63.

811 48. Harrison XA. Using observation-level random effects to model overdispersion in count data in
812 ecology and evolution. PeerJ. PeerJ Inc.; 2014;2:e616.

813 49. Jakobsson M, Edge MD, Rosenberg NA. The Relationship Between FST and the Frequency of the
814 Most Frequent Allele. Genetics. 2013;193:515–28.

815 50. Toleman MA, Rolston K, Jones RN, Walsh TR. blaVIM-7, an Evolutionarily Distinct Metallo-β-
816 Lactamase Gene in a *Pseudomonas aeruginosa* Isolate from the United States. ANTIMICROB AGENTS
817 CHEMOTHER. :48:329-332.

818 51. Manchanda V, Sanchaita S, Singh N. Multidrug Resistant Acinetobacter. J Glob Infect Dis.
819 2010;2:291–304.

820 52. Vandewalle JL, Goetz GW, Huse SM, Morrison HG, Sogin ML, Hoffmann RG, et al. *Acinetobacter*,
821 *Aeromonas* and *Trichococcus* populations dominate the microbial community within urban sewer
822 infrastructure. EnvironMicrobiol. 2012;14:2538–52.

823 53. Fisher JC, Levican A, Figueras MJ, McLellan SL. Population dynamics and ecology of *Arcobacter* in
824 sewage. FrontMicrobiol. 2014;5:525.

825 54. Ferreira S, Fraqueza MJ, Queiroz JA, Domingues FC, Oleastro M. Genetic diversity, antibiotic
826 resistance and biofilm-forming ability of *Arcobacter butzleri* isolated from poultry and environment from
827 a Portuguese slaughterhouse. IntJFood Microbiol. 2013;162:82–8.

828 55. Batovska J, Mee PT, Lynch SE, Sawbridge TI, Rodoni BC. Sensitivity and specificity of
829 metatranscriptomics as an *arbovirus* surveillance tool. Sci Rep. Nature Publishing Group; 2019;9:19398.

830 56. Sivalingam P, Poté J, Prabakar K. Extracellular DNA (eDNA): Neglected and Potential Sources of
831 Antibiotic Resistant Genes (ARGs) in the Aquatic Environments. Pathogens. 2020;9:874.

832 57. Eramo A, Medina WRM, Fahrenfeld NL. Viability-based quantification of antibiotic resistance genes
833 and human fecal markers in wastewater effluent and receiving waters. The Science of the total
834 environment. NIH Public Access; 2019;656:495.

835 58. Haines AS, Jones K, Cheung M, Thomas CM. The *IncP-6* plasmid *Rms149* consists of a small
836 mobilizable backbone with multiple large insertions. J Bacteriol. 2005;187:4728–38.

837 59. Matter D, Rossano A, Sieber S, Perreten V. Small multidrug resistance plasmids in *Actinobacillus*
838 *porcitonsillarum*. Plasmid. 2008;59:144–52.

839 60. Jensen LB, Frimodt-Moller N, Aarestrup FM. Presence of erm gene classes in gram-positive bacteria
840 of animal and human origin in Denmark. FEMS MicrobiolLett. 1999;170:151–8.

841 61. Jensen LB, Garcia-Migura L, Valenzuela AJS, Løhr M, Hasman H, Aarestrup FM. A classification system
842 for plasmids from *enterococci* and other Gram-positive bacteria. Journal of Microbiological Methods.
843 2010;80:25–43.

844 62. Palmer KL, Kos VN, Gilmore MS. Horizontal Gene Transfer and the Genomics of *Enterococcal*
845 Antibiotic Resistance. Curr Opin Microbiol. 2010;13:632–9.

846 63. Popowska M, Krawczyk-Balska A. Broad-host-range *IncP-1* plasmids and their resistance potential.
847 Frontiers in Microbiology. 2013;4;Article 44.

848 64. Røder HL, Hansen LH, Sørensen SJ, Burmølle M. The impact of the conjugative *IncP-1* plasmid *pKJK5*
849 on multispecies biofilm formation is dependent on the plasmid host. FEMS Microbiol Lett.
850 2013;344:186–92.

851 65. Wu J-R, Shieh HK, Shien J-H, Gong S-R, Chang P-C. Molecular characterization of plasmids with
852 antimicrobial resistant genes in avian isolates of *Pasteurella multocida.* Avian Dis. 2003;47:1384–92.

853 66. Karygianni L, Ren Z, Koo H, Thurnheer T. Biofilm Matrixome: Extracellular Components in Structured
854 Microbial Communities. Trends in Microbiology. 2020;28:668–81.

855 67. Gu C, Gao P, Yang F, An D, Munir M, Jia H, et al. Characterization of extracellular polymeric
856 substances in biofilms under long-term exposure to ciprofloxacin antibiotic using fluorescence
857 excitation-emission matrix and parallel factor analysis. Environ Sci Pollut Res. 2017;24:13536–45.

858 68. Hannan S, Ready D, Jasni AS, Rogers M, Pratten J, Roberts AP. Transfer of antibiotic resistance by
859 transformation with eDNA within oral biofilms. FEMS Immunology & Medical Microbiology.
860 2010;59:345–9.

861 69. Loustau E, Leflaive J, Boscus C, Amalric Q, Ferriol J, Oleinikova O, et al. The Response of Extracellular
862 Polymeric Substances Production by Phototrophic Biofilms to a Sequential Disturbance Strongly
863 Depends on Environmental Conditions. Frontiers in Microbiology. 2021;12; article 742027.

864 70. Okshevsky M, Meyer RL. The role of extracellular DNA in the establishment, maintenance and
865 perpetuation of bacterial biofilms. Critical Reviews in Microbiology. Taylor & Francis; 2015;41:341–52.

866 71. Wilton M, Charron-Mazenod L, Moore R, Lewenza S. Extracellular DNA Acidifies Biofilms and Induces
867 Aminoglycoside Resistance in *Pseudomonas aeruginosa*. Antimicrobial Agents and Chemotherapy.
868 American Society for Microbiology; 2015;60:544–53.

869 72. Doroshenko N, Tseng BS, Howlin RP, Deacon J, Wharton JA, Thurner PJ, et al. Extracellular DNA
870 impedes the transport of vancomycin in *Staphylococcus epidermidis* biofilms preexposed to
871 subinhibitory concentrations of vancomycin. AntimicrobAgents Chemother. 2014;58:7273–82.

872 73. Lewenza S. Extracellular DNA-induced antimicrobial peptide resistance mechanisms in *Pseudomonas*
873 *aeruginosa*. Front Microbiol. 2013;4:21.

874 74. Che Y, Yang Y, Xu X, Břinda K, Polz MF, Hanage WP, et al. Conjugative plasmids interact with insertion
875 sequences to shape the horizontal transfer of antimicrobial resistance genes. Proc Natl Acad Sci USA.
876 2021;118:e2008731118.

877 75. Varani A, He S, Siguier P, Ross K, Chandler M. The *IS6* family, a clinically important group of insertion
878 sequences including *IS26*. Mobile DNA. 2021;12:11.

879

880